

**New Amidated 3,6-diphenylated Imidazopyridazines with Potent Antiplasmodium Activity are Dual Inhibitors of *Plasmodium* phosphatidylinositol-4-kinase and cGMP-dependent protein kinase**

Peter Mubanga Cheuka,<sup>†,‡</sup> Luyanda Centani,<sup>†</sup> Lauren B. Arendse,<sup>Ω,Π</sup> Stephen Fienberg,<sup>†,Π</sup> Lynn Wambua,<sup>†</sup> Shoneeze S. Renga,<sup>†</sup> Godwin Akpeko Dziwornu,<sup>†</sup> Malkeet Kumar,<sup>†</sup> Nina Lawrence,<sup>∞</sup> Dale Taylor,<sup>∞</sup> Sergio Wittlin,<sup>||,⊥</sup> Dina Coertzen,<sup>§</sup> Janette Reader,<sup>§</sup> Mariette van der Watt,<sup>§</sup> Lyn-Marie Birkholtz<sup>§</sup> and Kelly Chibale<sup>\*,†,Ω,Π</sup>

<sup>†</sup>Department of Chemistry, University of Cape Town, Rondebosch 7701, Cape Town, South Africa.

<sup>‡</sup>Department of Chemistry, University of Zambia, Great East Road Campus, P.O Box 32379, Lusaka, Zambia.

<sup>∞</sup>Drug Discovery and Development Centre (H3D), Division of Clinical Pharmacology, Department of Medicine, University of Cape Town, Observatory 7925, Cape Town, South Africa.

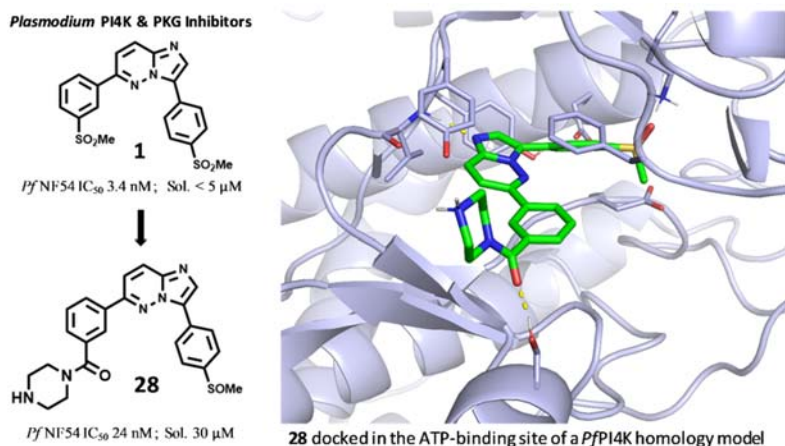
<sup>||</sup>Swiss Tropical and Public Health Institute, Socinstrasse 57, 4002 Basel, Switzerland.

<sup>⊥</sup>University of Basel, 4003 Basel, Switzerland.

<sup>§</sup>Department of Biochemistry, Genetics and Microbiology, Institute for Sustainable Malaria Control, University of Pretoria, Hatfield, Pretoria 0028, South Africa.

<sup>Ω</sup>Institute of Infectious Disease and Molecular Medicine, University of Cape Town, Rondebosch 7701, Cape Town, South Africa.

<sup>Π</sup>Drug Discovery and Development Centre (H3D) and South African Medical Research Council Drug Discovery and Development Research Unit, University of Cape Town, Rondebosch 7701, Cape Town, South Africa.



**Synopsis:** One of the most potent compounds in cellular assays, **28**, which also showed the strongest dual inhibition of PI4K and PKG sits in the ATP-binding site of a *Pf*PI4K homology model. This strategy is sustainable because: 1) It paves a way for less costly and more environmentally-friendly target-based optimization of the imidazopyridazine series; 2) Targeting two kinases could give rise to antimalarials with less propensity for resistance.

**ABSTRACT:** Recent studies on 3,6-diphenylated imidazopyridazines have demonstrated impressive *in vitro* activity and *in vivo* efficacy in mouse models of malaria infection. Herein, we report the synthesis and antiparasitoidium evaluation of a new series of amidated analogues and demonstrate that these compounds potently inhibit *Plasmodium* phosphatidylinositol-4-kinase (PI4K) type IIIβ while moderately inhibiting cyclic guanine monophosphate (cGMP)-dependent protein kinase (PKG) activity *in vitro*. Using *in silico* docking, we predict key binding interactions for these analogues within the adenosine triphosphate (ATP)-binding site of PI4K and PKG, paving the way for structure-based optimization of imidazopyridazines targeting both *Plasmodium* PI4K and PKG. While several derivatives showed low nanomolar antiparasitoidium activity (IC<sub>50</sub> < 100 nM), parent compounds **1** and **2** as well as the piperazine analogue **28** resulted in the strongest dual PI4K and PKG inhibition. The compounds also demonstrated transmission-blocking potential, evident from their potent inhibition of early-

and late-stage gametocytes. Finally, the current compounds generally showed improved aqueous solubility and reduced hERG (human *ether-a-go-go*-related gene) channel inhibition.

**KEYWORDS:** *antiplasmodium, antimalarial, imidazopyridazines, malaria, phosphatidylinositol-4-kinase (PI4K), cGMP-dependent protein kinase (PKG)*

There were 228 million malaria cases and 405,000 associated deaths in 2018 according to estimates by the World Health Organization (WHO).<sup>1</sup> Of all malaria cases and deaths, 93 and 94% respectively occurred in the WHO African region. Children under the age of 5 years are particularly prone to infection, illness and death accounting for 67% of all malaria deaths reported in 2018 globally. There are currently five species of protozoan parasites of the genus *Plasmodium* known to infect humans via the bites of infected female *Anopheles* mosquitoes. These include *P. falciparum*, *P. vivax*, *P. ovale*, *P. malariae* and *P. knowlesi* with the first two being the deadliest.

Malaria control efforts have been undermined by the emergence of widespread resistance to once effective treatment options such as chloroquine and sulfadoxine-pyrimethamine.<sup>2-5</sup> Even more concerning, in the Greater Mekong sub-region, 5 countries including Cambodia, Lao People's Democratic Republic, Myanmar, Thailand and Vietnam have reported emerging resistance to artemisinins, the main ingredients in currently recommended artemisinin combination therapies (ACTs). Worryingly, the failure rate of ACT-based treatments such as dihydroartemisinin – piperaquine for *P. falciparum* malaria infections in the North-Eastern part of Thailand has been found to be as high as 93%. Recently, the *Pfkelch13* R561H mutation was identified in 19 of 257 (7.4%) patients in Rwanda which could drive artemisinin resistance potentially compromising the continued success of antimalarial chemotherapy in Africa.<sup>6</sup> Therefore, there is a critical need to direct more research efforts into new, structurally diverse

and affordable antimalarial drugs with novel modes of action in an effort to circumvent the threat of resistance to first line treatment options.

The imidazopyridazine scaffold has been associated with a myriad of pharmacological properties,<sup>7-10</sup> while its antimalarial potential has also been explored.<sup>11-14</sup> Antiplasmodium imidazopyridazine compounds have also been previously reported to independently target PI4K<sup>14</sup> and PKG<sup>15</sup> (Figure 1). These enzymes are essential to multiple stages of the parasite life cycle and have emerged as promising antimalarial drug targets.<sup>14,16-18</sup> In addition to asexual blood-stage activity, *Plasmodium* PI4K and PKG inhibitors have shown the potential to block transmission and offer liver stage protection. The 2-aminopyridine drug candidate **MMV390048**, the first *Plasmodium* kinase inhibitor to enter clinical development for the treatment of malaria, targets *Plasmodium* PI4K.<sup>19</sup>

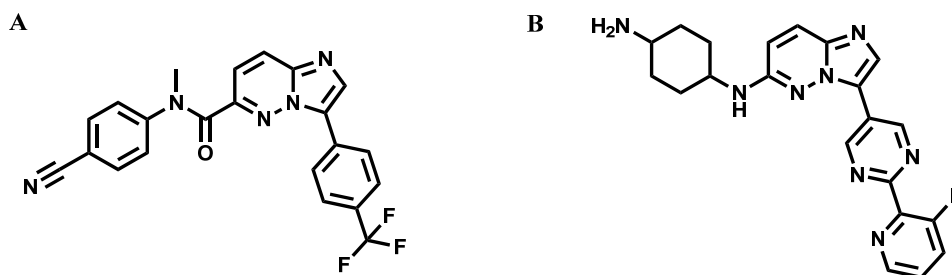
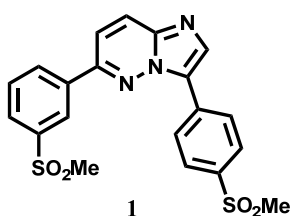


**Figure 1.** A) *Plasmodium* PI4K inhibitor (KAI715),<sup>14</sup> B) *Plasmodium* PKG inhibitor.<sup>15</sup>

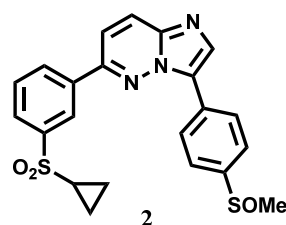
High-throughput screening of a BioFocus DPI SoftFocus kinase library identified the 3,6-diarylated congener with potent *in vitro* antiplasmodium activity and good *in vivo* antimalarial efficacy.<sup>20</sup> The optimization of the identified hit compounds through a phenotypically-driven medicinal chemistry campaign revealed, among others, the lead compound **1** (Figure 2). This compound was characterized by sub-optimal solubility (< 5  $\mu\text{M}$  at pH 6.5) and a serious hERG liability ( $\text{IC}_{50} = 0.9 \mu\text{M}$ ) raising concerns around potential cardiotoxicity. Subsequent analogues showed improved *in vivo* antimalarial efficacy (for

example, **2** in figure 2) although sub-optimal solubility and hERG inhibition liabilities remained an issue.

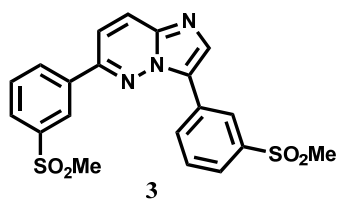
More recently, we have reported a different set of imidazopyridazine analogues which were designed to detune hERG activity and improve aqueous solubility.<sup>21</sup> These include compounds **3** (which retained poor solubility and a hERG inhibition risk despite having potent antiplasmodium activity) and **4** (with excellent solubility and reduced hERG inhibition although *in vitro* antiplasmodium potency was compromised) (Figure 2). When the selectivity index values (hERG IC<sub>50</sub>/Pf IC<sub>50</sub>) are considered, the compromised *in vitro* antiplasmodium activity for compounds **3** and **4** still makes them poor candidates for further progression.



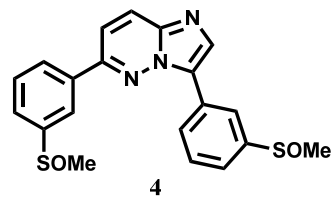
*Pf*NF54 IC<sub>50</sub> = 7.3 nM  
*Pf*K1 IC<sub>50</sub> = 6.3 nM  
*In vivo P. berghei* (po) at 4 × 50 mg/kg, 98%, 7 MSD<sup>a</sup>  
hERG IC<sub>50</sub> = 0.9 μM  
Solubility, pH 6.5 < 5 μM  
*Pv*PI4K IC<sub>50</sub> = 0.8 nM  
*Pf*PKG IC<sub>50</sub> = 120 nM



*Pf*NF54 IC<sub>50</sub> = 1.1 nM  
*In vivo P. berghei* (po) at 4 × 50 mg/kg, 99.8%, > 30 MSD<sup>a</sup>, 3 out of 3 mice cured  
Solubility, pH 6.5 < 5 μM  
*Pv*PI4K, %Inh.<sup>b</sup> @ 0.1 μM = 99.8  
*Pf*PKG, %Inh.<sup>b</sup> @ 10 μM = 99.5



*Pf*NF54 IC<sub>50</sub> = 31 nM  
Solubility, pH 6.5 < 5 μM  
hERG IC<sub>50</sub> = 2.35 μM



*Pf*NF54 IC<sub>50</sub> = 151 nM  
Solubility, pH 6.5 = 200 μM  
hERG IC<sub>50</sub> = 8.45 μM

**Figure 2.** Previously explored antimalarial imidazopyridazine analogues. <sup>a</sup>MSD, mean survival days; <sup>b</sup>Inh, inhibition.

To improve solubility in new analogues, we appended the amide functionality to the two phenyl rings attached to the imidazopyridazine core-scaffold (see analogues **5** – **30** in schemes 1 and 2). While all the final target compounds contained an amide bond, which is water solubilizing in its own right, some of these [**6** – **10**, **14** – **16** (Scheme 1), **19** – **21**, **23**, **27**, **28** and **30** (Scheme 2)] were designed to possess additional water solubilizing groups on the amide substituents. While introducing structural changes on the right-hand side phenyl ring, we fixed a 3-methylsulfinylphenyl group on the left-hand side of the core-scaffold. When related changes were made on the left-hand side phenyl ring, a 4-methylsulfinylphenyl group was fixed on the right-hand side of the core-scaffold. This substitution pattern on the two phenyl rings was motivated by earlier studies which have found these two positions optimal for antiplasmodium potency.<sup>20–22</sup> It was further reasoned that since sulfoxide groups are stronger hydrogen bond acceptors than sulfones,<sup>23</sup> sulfoxide substitution could further encourage water solubility. For comparison purposes, a sulfone version of **11**, compound **18**, was also generated.

The mechanism of action of antimalarial imidazopyridazines reported from our laboratories has, to date, not been elucidated. Given the reported inhibition of *Plasmodium* PI4K and PKG by related compounds based on the same scaffold, these kinases were explored as potential targets for this series. In this regard, *in vitro* kinase inhibition assays using recombinantly expressed *P. vivax* PI4K (*Pv*PI4K) and *P. falciparum* PKG (*Pf*PKG) were carried out on selected compounds, including previously published compounds **1** and **2**.

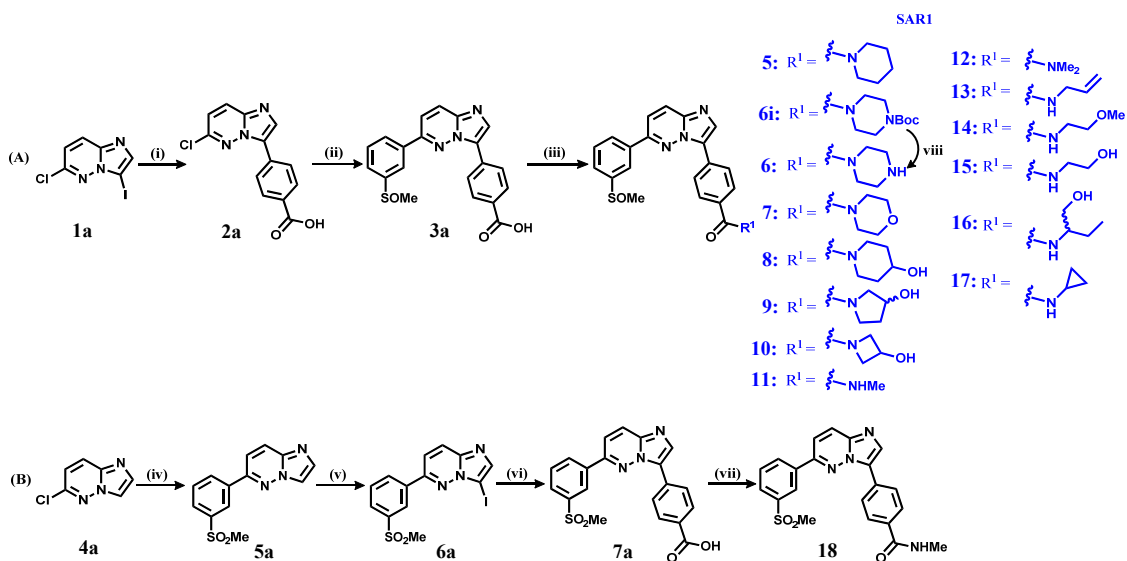
## RESULTS AND DISCUSSION

### Chemistry

Analogues **5** – **18** were synthesized according to Scheme 1. The target compounds **5** – **17** were realised following scheme 1A while compound **18** was obtained using scheme 1B. The dihalogenated precursor **1a** was synthesised according to a previously described method.<sup>21</sup>

Two sequential Suzuki-Miyaura coupling reactions on this intermediate delivered the benzoic acid intermediate **3a** in moderate yield (59%).<sup>20</sup> The target compounds **5** and **7 – 17** were then obtained in poor to good yields (5 – 69%) using an n-propylphosphonic anhydride (T3P)-mediated acid amine coupling in presence of *N,N*-Diisopropylethylamine (DIPEA).<sup>24</sup> The sulfone target compound **18** was synthesized from a different chloro-substituted intermediate **4a** (Scheme 1B). A previously described literature procedure was used to synthesize intermediate **4a**.<sup>21</sup> A Suzuki-Miyaura cross coupling reaction on this intermediate gave a phenylated intermediate **5a** in 63% yield. This was followed by a regioselective electrophilic aromatic iodination<sup>20</sup> and a subsequent Suzuki-Miyaura coupling to deliver a benzoic acid intermediate **7a** in 41% yield. Finally, a T3P-promoted acid amine coupling in presence of DIPEA delivered the amide target compound **18** in poor yield (17%). Compound **6** required an extra step – it was uniquely obtained following a boc-deprotection of its amide intermediate **6i**.<sup>25</sup>

**Scheme 1. General Synthetic Approach for Analogues 5 – 18<sup>a</sup>**

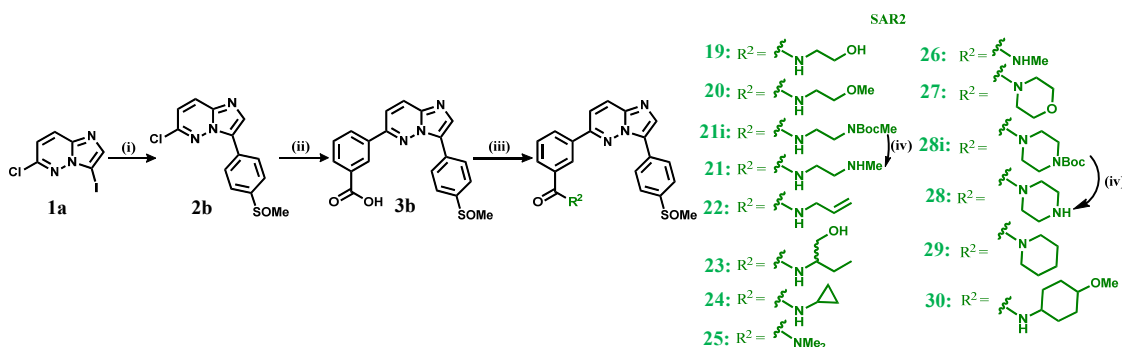


<sup>a</sup>Reagents and reaction conditions: (i) 4-carboxyphenylboronic acid, Pd(PPh<sub>3</sub>)<sub>2</sub>Cl<sub>2</sub>, 1 M aq K<sub>2</sub>CO<sub>3</sub>, DMF, 80 °C, 12 h, 53%; (ii) 3-methylsulfinylphenylboronic acid, Pd(PPh<sub>3</sub>)<sub>2</sub>Cl<sub>2</sub>, 1 M aq K<sub>2</sub>CO<sub>3</sub>, DMF, 100 °C, 16 h, 59%; (iii)

appropriate amine, 50% T3P in DMF (for **5**, **6i** and **7 – 12**), 50% T3P in ethyl acetate (for **13 – 17**), DIPEA, DMF (for **5**, **6i**, **7 – 10** and **13 – 17**), DCM (for **11** and **12**), 50 °C (for **5**, **6i**, **7 – 10** and **13 – 17**), rt (for **11** and **12**), 3 – 16 h, 5 – 69%; (iv) 3-methylsulfonylphenylboronic acid, Pd(PPh<sub>3</sub>)<sub>2</sub>Cl<sub>2</sub>, 1 M aq K<sub>2</sub>CO<sub>3</sub>, DMF, 100 °C, 19 h, 63%; (v) *N*-iodosuccinimide (NIS), DMF, 35 °C, 6 d, 87%; (vi) 4-carboxyphenylboronic acid, Pd(PPh<sub>3</sub>)<sub>2</sub>Cl<sub>2</sub>, 1 M aq K<sub>2</sub>CO<sub>3</sub>, DMF, 80 °C, 15 h, 41%; (vii) methylamine hydrochloride, 50% T3P in ethyl acetate, DIPEA, DMF, 50 °C, 3 h, 17%; (viii) trifluoroacetic acid, DCM, rt, 15 min.

The second set of analogues, **19 – 30**, were synthesized following a straightforward synthetic approach shown in scheme 2. Two Suzuki-Miyaura cross coupling reactions were sequentially carried out to give the key benzoic acid intermediate **3b**. This intermediate was then amidated in presence of T3P and DIPEA to furnish the amide intermediate and target compounds **19**, **20**, **21i**, **22 – 27**, **28i**, **29** and **30** in poor to good yields (4 – 67%). The target compounds **21** and **28** were obtained from their boc-protected precursors via boc-deprotection facilitated by HCl.

**Scheme 2. General Synthetic Approach for Analogues 19 – 30<sup>a</sup>**



<sup>a</sup>Reagents and reaction conditions: (i) 4-methylsulfonylphenylboronic acid, Pd(PPh<sub>3</sub>)<sub>2</sub>Cl<sub>2</sub>, 1 M aq K<sub>2</sub>CO<sub>3</sub>, DMF, 80 °C, 14 h, 77%; (ii) 3-carboxyphenylboronic acid, Pd(PPh<sub>3</sub>)<sub>2</sub>Cl<sub>2</sub>, 1 M aq K<sub>2</sub>CO<sub>3</sub>, 1,4-dioxane, 100 °C, 15 h, 68%; (iii) appropriate amine, 50% T3P in ethyl acetate, DIPEA, DMF (for **19**, **20**, **21i**, **26**, **27** and **28i**), 1,4-dioxane (for **22 – 25**, **29** and **30**), 50 °C (for **19**, **20**, **21i**, **26**, **27** and **28i**), 30 °C (for **22 – 25**, **29** and **30**), 1 – 21 h, 4 – 67%; (iv) 4 M HCl in 1,4-dioxane, DCM, rt, 20% (**28**) and 30% (**21**).

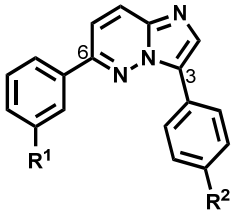
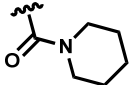
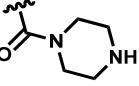
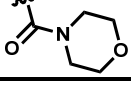
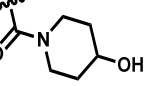
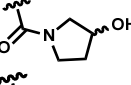
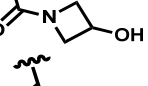
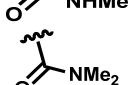
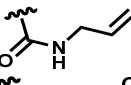
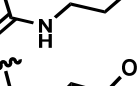
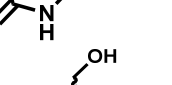
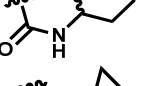
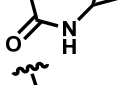


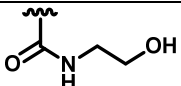


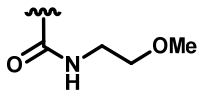
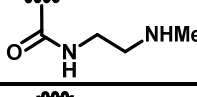
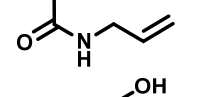
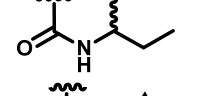
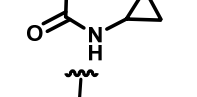
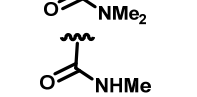
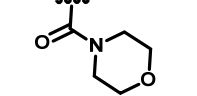
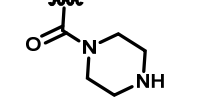
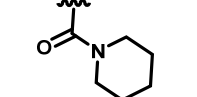
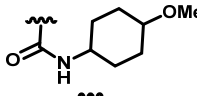
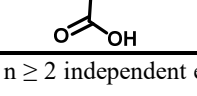
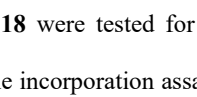
### ***In vitro* Asexual Blood Stage Antiplasmodium Activity and Solubility Profiling.**

The initial phase of our SAR studies focused on introducing amide functionalities at the *para* position of the phenyl ring on the right-hand side of the core scaffold while fixing a sulfoxide group at the *meta* position of the phenyl ring on the left-hand side (SAR1, analogues **5** – **17**, Table 1). In addition to uncovering important structure-activity relationships, this set of modifications identified compounds with a combination of good antiplasmodium activity and solubility. Furthermore, all compounds tested on both the NF54 and K1 strains of *P. falciparum* did not show significant differences between potencies across the two strains. (Table S1 in the supporting information). All chiral compounds were evaluated as racemic and diastereomeric mixtures as no chiral separation was performed during the synthesis.

Compared to analogue **5** ( $IC_{50} = 0.317 \mu M$ ), the piperazine analogue **6** ( $IC_{50} = 0.103 \mu M$ ) was found to be 3-fold more potent, indicating the importance of a hydrogen bond donor in the six-membered ring. Hydroxylation of the piperidine ring also appears favourable towards antiplasmodium potency (cf., **5** and **8**). Analogues **8** ( $IC_{50} = 0.106 \mu M$ ), **9** ( $IC_{50} = 0.055 \mu M$ ) and **10** ( $IC_{50} = 0.097 \mu M$ ) were shown to be roughly equipotent, suggesting hydroxylated 4-6 membered rings are tolerated in this position. The sulfone analogue of **9**, previously reported by Le Manach *et al.*,<sup>22</sup> was also found to be highly potent ( $IC_{50} = 0.018 \mu M$ ) suggesting only a single hydrogen bond acceptor in this position is required for antiplasmodium activity.

Table 1. *In vitro* Activity Against Asexual Blood Stage *P. falciparum* NF54, PvPI4K and PfPKG and Solubility

						
Code	R <sup>1</sup>	R <sup>2</sup>	<i>P. f</i> NF54 IC <sub>50</sub> , μM <sup>a,b</sup>	Solubility, μM <sup>c</sup>	% PvPI4K inh. @ 0.1 μM (SD) <sup>d</sup>	% PfPKG inh. @ 10 μM (SD) <sup>d</sup>
5	SOMe		0.317	70	83 (1)	80.7 (0.1)
6	SOMe		0.103	200	95.4 (0.7)	58.0 (0.2)
7	SOMe		0.162	75		
8	SOMe		0.106	170	96.0 (0.2)	31 (3)
9	SOMe		0.055	200		
10	SOMe		0.097	200	95.5 (0.8)	25.2 (0.9)
11	SOMe		0.067	195		
12	SOMe		0.146	200		
13	SOMe		0.141		95 (3)	49 (6)
14	SOMe		0.144	200 <sup>e</sup>	93 (3)	12.7 (0.1)
15	SOMe		0.371		94.7 (0.8)	29.8 (0.1)
16	SOMe		0.290	80 <sup>e</sup>	91 (1)	64.2 (0.1)
17	SOMe		0.209	200 <sup>e</sup>	88.4 (0.6)	46 (5)
18	SO <sub>2</sub> Me		0.019	5 <sup>e</sup>	99.8 (0.6)	75 (4)
19		SOMe	0.069	145	97 (2)	63 (2)

20		SOMe	0.198	200 <sup>e</sup>	97.4 (0.9)	46 (2)
21		SOMe	0.088	< 5	93.5 (0.7)	90.7 (0.02)
22		SOMe	0.094	200 <sup>e</sup>	95 (2)	64 (6)
23		SOMe	0.201		95 (6)	42 (1)
24		SOMe	0.284	200 <sup>e</sup>	94 (3)	60 (3)
25		SOMe	0.131		98.0 (0)	46 (5)
26		SOMe	0.012	< 5	99 (1)	52 (15)
27		SOMe	0.016	200	99.7 (0.1)	47.3 (8)
28		SOMe	0.024	30	98.6 (0.4)	95 (6)
29		SOMe	0.012	200 <sup>e</sup>	99.2 (0.7)	78.1 (0.6)
30		SOMe	6.00	< 5 <sup>e</sup>	78.4 (0.9)	-3 (3)
3b		SOMe	8.87	< 5		

<sup>a</sup>Mean from  $n \geq 2$  independent experiments (Individual  $IC_{50}$  values differed by  $\leq 2$ -fold); Compounds **5**, **7** – **12**, **14**, **17** and **18** were tested for *in vitro* asexual blood stage antiplasmodium activity using a modified [<sup>3</sup>H]-hypoxanthine incorporation assay while a parasite lactate dehydrogenase assay was employed for compounds **6**, **13**, **15**, **16**, **19** – **30** and **3b**.

<sup>b</sup>Artesunate [ $IC_{50} = 4.0$  nM (NF54)] and chloroquine [ $IC_{50} = 16$  nM (NF54)] were used as reference drugs.

<sup>c</sup>All values except those marked with a footnote citation “<sup>e</sup>” were determined using an HPLC-based miniaturized shake flask method at pH 6.5.

<sup>d</sup>Percentage enzyme inhibition in the presence of 10  $\mu$ M ATP, mean of  $n = 2$  independent experiments each carried out in triplicate; SD, standard deviation.

Blank cells = data not available.

<sup>e</sup>Determined using kinetic (turbidimetric) solubility assay at pH 7.4.

In addition to tertiary amides with cyclic substituents (**5** – **10**) discussed thus far, the SAR was further expanded upon by exploring secondary amides with open chain (**11** and **13** – **16**) and cyclic (**17**) substituents. Apart from a mono-*N*-methylated analogue **11**, which exhibited strong antiplasmodium potency ( $IC_{50} = 0.067 \mu\text{M}$ ), the secondary amides were generally relatively less potent ( $IC_{50} = 0.141 - 0.371 \mu\text{M}$ ). When the amide nitrogen in **11** was methylated to **12**, the antiplasmodium potency was reduced by 2-fold, suggesting the secondary amide acts as a hydrogen bond donor. Interestingly, the sulfone analogue of **11**, **18** ( $IC_{50} = 0.019 \mu\text{M}$ ) was highly potent with superior activity to all the secondary amides explored.

Furthermore, compared to the poorly soluble lead compound **1** ( $< 5 \mu\text{M}$ ), all sulfoxide-substituted analogues, where the solubility was determined (**5** – **12**, **14**, **16** and **17**), showed substantial improvements in solubility ( $70 - 200 \mu\text{M}$ ) (Table 1). Conversely, while analogue **11** displayed excellent solubility ( $195 \mu\text{M}$ ), its sulfone analogue **18** was poorly soluble ( $5 \mu\text{M}$ ). The superior solubility of the sulfoxide analogue **11** is expected since sulfoxides are stronger hydrogen bond acceptors than sulfones.<sup>23</sup> This finding is in agreement with previously published solubility profiles comparing sulfone and sulfoxide derivatives of imidazopyridazines.<sup>21,22</sup>

We further decided to expand the SAR by generating analogues with an amide functionality at the *meta* position of the left-hand side phenyl ring while fixing a 4-methylsulfinylphenyl group on the imidazole portion of the core scaffold (SAR2, **19** – **30**, Table 1). Compared to SAR1, modifications in this SAR set were generally well tolerated with most analogues exhibiting nanomolar antiplasmodium activity ( $IC_{50} = 0.012 - 0.094 \mu\text{M}$ ). There are also important changes in antiplasmodium activity accompanying structural changes worth mentioning. An *O*-methylation from **19** ( $IC_{50} = 0.069 \mu\text{M}$ ) to **20** ( $IC_{50} = 0.198 \mu\text{M}$ ) resulted in a near 3-fold reduction in antiplasmodium activity. Compound **19** was also found to be equipotent to its previously reported<sup>20</sup> sulfone congener suggesting that only a single

hydrogen bond acceptor in the sulfoxide is necessary for antiplasmodium activity. Compound **23** ( $IC_{50} = 0.201 \mu\text{M}$ ), which is an ethylated version of **19**, also exhibited a near 3-fold reduction in antiplasmodium potency. The *N,N*-dimethylated analogue **25** ( $IC_{50} = 0.131 \mu\text{M}$ ) was 11-fold less active than its corresponding *N*-monomethylated form **26** ( $IC_{50} = 0.012 \mu\text{M}$ ), mirroring the trend observed for the analogues **11** and **12** (SAR1). Interestingly, analogues whose amide nitrogen belongs to a six-membered ring such as **27** ( $IC_{50} = 0.016 \mu\text{M}$ ), **28** ( $IC_{50} = 0.024 \mu\text{M}$ ) and **29** ( $IC_{50} = 0.012 \mu\text{M}$ ) were nearly equipotent indicating both polar and non-polar groups are tolerated at position 4 on these rings. In previous studies,<sup>20</sup> the sulfone forms of the piperazine (**28**) and piperidine (**29**) analogues have also been shown to be highly potent, another example demonstrating sulfones and sulfoxides to be equipotent in this position. Lastly, amidation with 4-methoxycyclohexylamine to give compound **30** ( $IC_{50} = 6.00 \mu\text{M}$ ) caused a complete loss of potency. The free carboxylic acid **3b** ( $IC_{50} = 8.87 \mu\text{M}$ ) was also highly inactive suggesting a negatively charged group in this position is detrimental to antiplasmodium activity. Compared to the previously reported<sup>20</sup> lead compound **1**, most compounds in SAR2 displayed an improvement in aqueous solubility. In this regard, compounds **19**, **20**, **22**, **24**, and **27 – 29** were found to be 6 – 40-fold more soluble than **1**.

Selected analogues were also evaluated for their potential cardiotoxicity risk by testing their inhibition of the hERG channel stably expressed in the Chinese Hamster Ovarian (CHO) cell line (Table S2 in the supporting information). Apart from analogue **5**, which weakly inhibited the hERG channel ( $IC_{50} = 9 \mu\text{M}$ ), the remainder, **7 – 12**, **21** and **26 – 28**, displayed < 50% inhibition at 10  $\mu\text{M}$  (the highest inhibitor concentration tested), with all compounds demonstrating wide safety margins. In addition, this series displayed low *in vitro* cytotoxicity, with all analogues tested exhibiting good selectivity indexes (CHO  $IC_{50}/P. f$  NF54  $IC_{50} = 275 - > 2381$ ) (Table S2 in the supporting information).

***In vitro* Transmission Blocking Activity against *P. falciparum* Gametocytes and Gametes.** Compounds from SAR1 and SAR2, **13-18, 20, 22, 24, 28** and **29**, were screened for activity against *in vitro* cultured early- and late-stage *P. falciparum* NF54 gametocytes. Compounds were initially investigated for their % inhibition of early- and late-stage gametocytes at two concentrations (5 and 1  $\mu$ M) (Table S3 in the supporting information). Compounds that exhibited good activity (> 70% inhibition at 5  $\mu$ M and > 50% inhibition at 1  $\mu$ M) in these dual-point assays were then prioritized for full IC<sub>50</sub> determination. The SAR1 analogue, compound **18**, was the only compound with IC<sub>50</sub> values in the nM range against both early-stage (IC<sub>50</sub> = 558.7  $\pm$  73 nM) and late-stage (IC<sub>50</sub> = 157.7  $\pm$  4.8 nM) gametocytes (Table 2). SAR2 analogues overall delivered more potent gametocytocidal compounds: **22** and **28**, were active at sub-micromolar concentrations against both early- and late-stage gametocytes while compound **29** was potent at < 100 nM against both gametocyte stages (early-stage gametocytes IC<sub>50</sub> = 22.8  $\pm$  7.3 nM, and late-stage gametocytes IC<sub>50</sub> = 42.3  $\pm$  3.5 nM, Table 2). The transmission-blocking potential of compounds active against late-stage gametocytes (IC<sub>50</sub>s < 1  $\mu$ M) was confirmed by evaluating their activity against male gametes. **18, 22, 28** and **29** were all able to significantly (> 90% inhibition) prevent male gamete exflagellation (Table 2).

**Table 2. Sexual Stage *In vitro* Activity Against *P. falciparum* NF54**

Code	R <sup>1</sup>	R <sup>2</sup>	<i>P. f</i> EG IC <sub>50</sub> , μM (SEM) <sup>k</sup>	<i>P. f</i> LG IC <sub>50</sub> , μM (SEM) <sup>a</sup>	% <i>P. f</i> gamete inh. @ 2 μM <sup>b</sup>
18	SO <sub>2</sub> Me		0.559 (0.073)	0.158 (0.0048)	90.3
20		SOMe		1.22 (0.20)	
22		SOMe	0.57 (0.05)	0.78 (0.04)	93.6
24		SOMe		1.00 (0.11)	
28		SOMe	0.39 (0.18)	0.12 (0.03)	96.8
29		SOMe	0.0228 (0.0073)	0.0423 (0.0035)	100.0

<sup>a</sup> IC<sub>50</sub> of early-stage gametocytes (EG) and late-stage gametocytes (LG), mean of n = 3 independent experiments each carried out in triplicate; SEM, standard error of the mean.

<sup>b</sup>Percentage male gamete exflagellation inhibition at 2 μM, n = 1.

Blank cells = data not available.

***In vitro Plasmodium* PI4K and PKG Inhibition.** Analogues from both SAR1 and 2 were screened *in vitro* for inhibition of recombinant *Pv*PI4K (PVX\_098050) and *Pf*PKG (PF3D7\_1436600) (Table 1). *Pv*PI4K and *Pf*PI4K (PF3D7\_0509800) kinase domains share 96% sequence identity and their ATP-binding sites are completely conserved making *Pv*PI4K a suitable surrogate for *Pf*PI4K. All analogues tested exhibited potent inhibition of *Pv*PI4K with 19/22 analogues showing > 90% inhibition at a concentration of 0.1 μM, providing a possible explanation for the potent antiplasmodium activity generally observed for this series. Several analogues also showed weak to moderate activity against *Pf*PKG.

Of the SAR1 analogues tested, **18**, the compound with the most potent antiplasmodium activity ( $IC_{50} = 0.019 \mu\text{M}$ ), also displayed the highest potency against *Pv*PI4K (99.8% inhibition at  $0.1 \mu\text{M}$  inhibitor concentration). All SAR2 analogues, other than **30**, displayed > 90% *Pv*PI4K inhibition when tested at  $0.1 \mu\text{M}$ . While analogue **30** displayed less potent whole cell activity than the others, it still exhibited 78.4% *Pv*PI4K inhibition at  $0.1 \mu\text{M}$  suggesting that other factors may be contributing to the observed poor whole cell activity. In addition to potent *Pv*PI4K activity, **21** and **28** also exhibited moderate activity against *Pf*PKG (90.7% and 95% inhibition respectively when tested at  $10 \mu\text{M}$ ) as was observed for compounds **1** and **2** (Figure 1).

***Plasmodium* PI4K and PKG In silico Docking Studies.** The 3,6-substituted imidazopyridazine scaffold is a well-established kinase ATP-binding site hinge binding moiety. It has been co-crystallised in complex with numerous kinases [protein data base (PDB) codes 4TXC, 4YMJ, 4YNE, 3BQR, 2PMN, 6S11] with the 1-N accepting a H-bond from a hinge backbone amide.<sup>26–28</sup> The imidazopyridazine scaffold has been observed to bind in two different orientations with the 3- and 6- substituents interacting with either the ribose pocket or the catalytic subsite.

There is no high-resolution structure of *Plasmodium* PI4K available, so a *Pf*PI4K homology model, built using a high-resolution human PI4KIII $\beta$  structure (4D0L)<sup>29</sup> as a template, was used for docking studies.<sup>30</sup> In contrast, the *Plasmodium* PKG structure is well-characterised.<sup>31</sup> For *Pf*PKG, only the apo structure (PDB code 5DYK) has been deposited in the PDB but six *Pv*PKG structures, including several structures with inhibitors bound within the ATP-binding site, are available.<sup>17,31</sup> Both *Pf*PKG and *Pv*PKG have identical ATP-binding sites, so a high-resolution inhibitor-bound *Pv*PKG structure (5EZR) was selected as a more suitable structure for modelling these compounds.



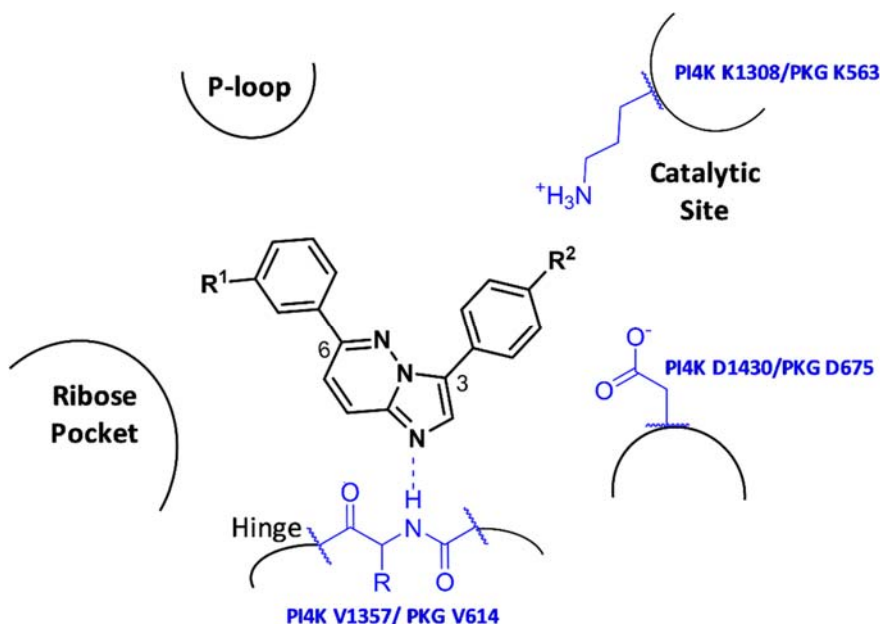


**Figure 3.** 2D schematic showing the general binding orientation of the 3,6-diarylated imidazopyridazine core within the ATP-binding site of *Pf*PI4K and *Pv*PKG. The conserved hinge-binding valine residue and the catalytic Lysine and Aspartate residues are shown in blue (*Pf*PI4K/*Pv*PKG).

In both kinases, the imidazopyridazine core was predicted to accept a H-bond from a backbone amide of the hinge with the 3-position substituent interacting with the conserved catalytic Lys and Asp residues and the 6-position substituent interacting with the ribose pocket (Figure 3). Many compounds in this series contained a chiral sulfoxide moiety at either the SAR1 position (**5-17**) or the SAR2 position (**22 – 30, 3b**) while only racemates were synthesised and evaluated. For the purposes of docking, every enantiomer/diastereomer of each compound was docked into both models. The (*S*)-sulfoxide was found to be greatly favored over the (*R*)-sulfoxide in the SAR1 and less so in the SAR2 position on both *Pf*PI4K and *Pv*PKG. In the SAR1 position, the (*S*)-sulfoxide is better positioned to accept more ribose pocket H-bonds, while in the SAR2 position, the (*S*)-sulfoxide is better configured to accept H-bonds from both the catalytic Lys and the backbone of the catalytic acid but with only a slight binding advantage over the (*R*)-enantiomer at this locus.

The potent PI4K inhibitor **10**, docks into the PI4K homology model with the 1-*N* accepting a H-bond from the backbone amide of Val1357 (Figure 4A). The 3-phenyl group sits in a hydrophobic pocket while its carboxamide carbonyl accepts a H-bond from the catalytic Lys1308. The azetidinol group donates an H-bond to the catalytic Asp1430. In the ribose pocket, the *meta* sulfoxide accepts hydrogen bonds from both Ser1365 and the backbone amide of Lys1369. In addition to strong H-bonds in these three kinase subsites, the three aromatic systems can form aromatic  $\pi$ -stacking interactions with Phe827 and Tyr1356, accounting for the particularly high potency of this series against PI4K.

In addition to PI4K inhibition, this 3,6-diarylated imidazopyridazine series displays weak to moderate inhibition of PKG. As observed in PI4K, analogue **10** accepts a hinge H-bond from the backbone amide of Val614 (Figure 4B). The 3-phenyl group sits in a similar hydrophobic pocket to that of PI4K, with the carboxamide carbonyl accepting a H-bond from the catalytic Lys563 and the backbone amide of the conserved catalytic Asp675. Unlike PI4K, PKG has a deeper so-called protein kinase back pocket (similar to the “affinity” pocket in lipid kinases)<sup>32</sup> which is accessible due to the presence of the small gatekeeper residue Thr611.<sup>33</sup> The azetidinol group extends into this back pocket participating in H-bonding with Glu582 and Lys563. The *meta* sulfoxide substituent in the 6-position phenyl does not interact favourably with the base of the ribose pocket of PKG due to the presence of two acids on either side of the pocket (Glu618 and Glu661), but instead forms a H-bond with the backbone amide of Arg542 in the P-loop. This, together with the lack of aromatic  $\pi$ -stacking interactions observed in PI4K, provides an explanation for the poor PKG inhibition observed for **10** (25.2% inhibition at 10  $\mu$ M).

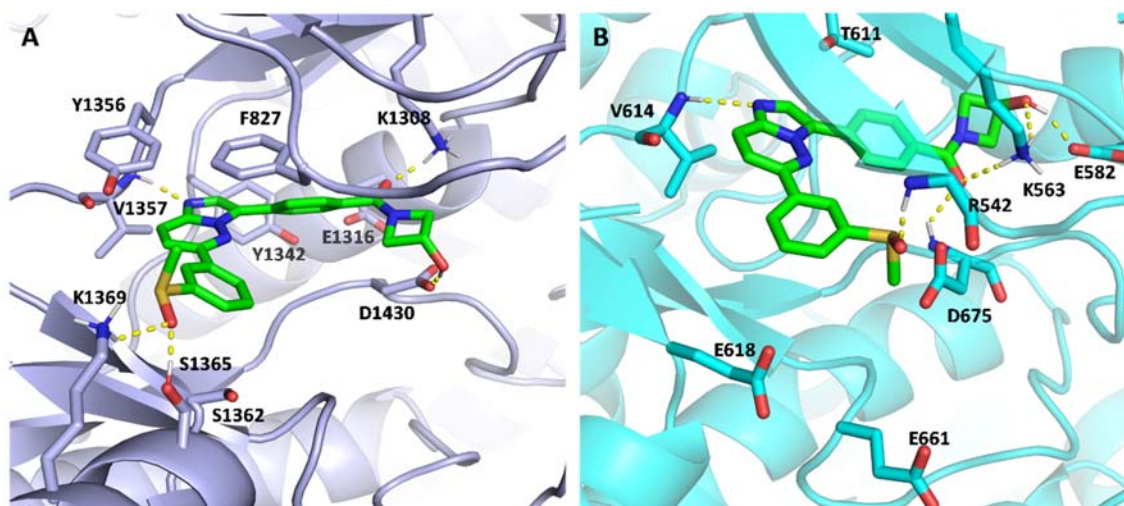


**Figure 4.** Analogue (*S*)-**10** (green) docked in the ATP-binding site of **A**) *Pf*PI4K homology model and **B**) *Pv*PKG (PDB code 5EZR). Hydrogen bonds are shown in yellow.

Compound **28** is the strongest PKG inhibitor in this series (95% inhibition at 10  $\mu$ M). It docks into PKG with the common hinge interaction and the *para* sulfoxide accepts H-bonds from both the catalytic Lys563 and the backbone amide of the catalytic Asp675 (Figure 5A). In the ribose pocket, the basic piperazine amide fits between the acids Glu661 and Asp675, donating a H-bond to Asn662. Substituting this basic piperazine with the morpholine of **27** replaces a basic charged N with a neutral acceptor O. Positioning this O between two acids is highly unfavourable and explains the loss of PKG activity observed for **27** (Figure 5A). In contrast to PKG, **27** and **28** are both strong inhibitors of PI4K. Both these compounds accept the same hinge H-bond and the same H-bond between the sulfoxide O and the catalytic Lys1308 in PI4K (Figure 5B). In the ribose pocket, the *meta* carboxamide in both compounds forms a H-bond with Ser1365. The PI4K ribose pocket is more solvent accessible than in PKG, thus tolerating both a basic piperazine and a neutral morpholine on the solvent edge. The morpholine is also capable of forming a H-bond with a solvent exposed Lys825 while the piperazine is free to interact with the solvent.

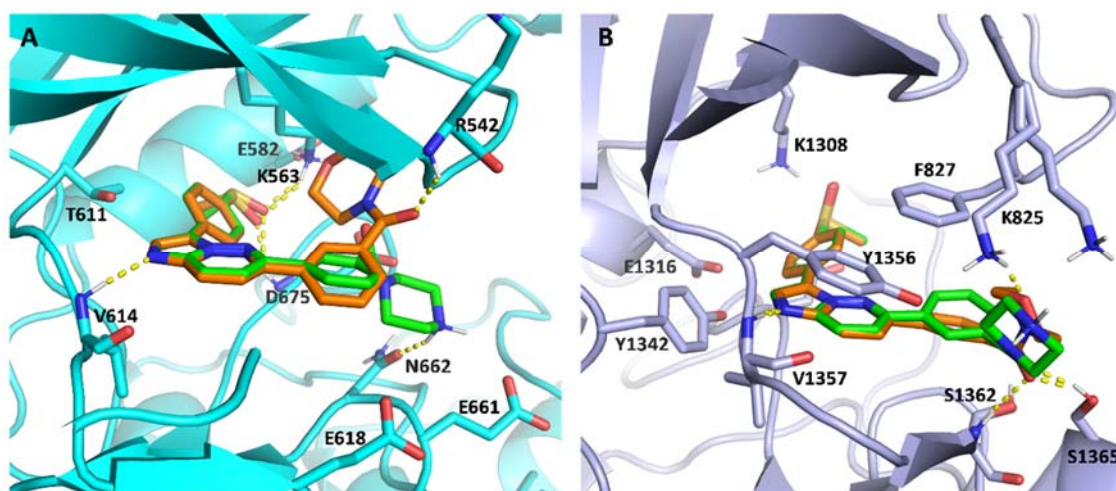


**Figure 5.** Analogue (S)-27 (orange) and (S)-28 (green) docked in the ATP-binding site of A) *Pv*PKG (PDB code 5EZR) and B) *P/PI4K* homology model. Hydrogen bonds are shown in yellow.

**Off-Target Human Kinase Inhibition.** To investigate the risk of off-target human kinase inhibition, a representative set of compounds was screened *in vitro* for inhibition of human PI4KIII $\beta$  (*Hu*PI4KIII $\beta$ ), the most closely related human orthologue of *Plasmodium* PI4K (Table 3).

**Table 3: Comparison of *in vitro* Inhibition of *Pv*PI4K and *Hu*PI4KIII $\beta$**

Compound	R <sup>1</sup>	R <sup>2</sup>	% <i>Pv</i> PI4K inh. @ 0.1 $\mu$ M (SD) <sup>m</sup>	% <i>Hu</i> PI4KIII $\beta$ inh. @ 1 $\mu$ M (SD) <sup>m</sup>
6	SOMe		95.4 (0.7)	54 (3)
8	SOMe		96.0 (0.2)	50 (3)

**Table 3: Comparison of *in vitro* Inhibition of *Pv*PI4K and *Hu*PI4KIII $\beta$  “continued”**

Compound	R <sup>1</sup>	R <sup>2</sup>	% <i>Pv</i> PI4K inh. @ 0.1 $\mu$ M (SD) <sup>m</sup>	% <i>Hu</i> PI4KIII $\beta$ inh. @ 1 $\mu$ M (SD) <sup>a</sup>
10	SOMe		95.5 (0.8)	32 (2)
18	SO <sub>2</sub> Me		99.8 (0.6)	92.96 (0.05)
21		SOMe	93.5 (0.7)	41 (2)
24		SOMe	94 (3)	75.5 (0.7)
26		SOMe	99 (1)	86.4 (0.4)
27		SOMe	99.7 (0.1)	82.5 (0.2)
28		SOMe	98.6 (0.4)	90.5 (0.1)
29		SOMe	99.2 (0.7)	95.5 (0.2)

<sup>m</sup>Percentage enzyme inhibition in the presence of 10  $\mu$ M ATP, mean of n = 2 independent experiments; SD, standard deviation.

Blank cells = data not available.

All 10 compounds displayed more potent activity against *Pv*PI4K than *Hu*PI4KIII $\beta$ , showing higher percentage *Pv*PI4K inhibition at 0.1  $\mu$ M inhibitor concentration than *Hu*PI4KIII $\beta$  inhibition at 1  $\mu$ M inhibitor concentration. Despite this, all 10 analogues showed moderate to potent inhibition of *Hu*PI4KIII $\beta$  at 1  $\mu$ M. Therefore, the *Hu*PI4KIII $\beta$  off-target activity is likely to be a hurdle for this series and will have to be addressed before the series can be taken forward. Of the 10 compounds in this subset, **8**, **10** and **21** were the most selective for *Pv*PI4K, displaying  $\leq 50\%$  *Hu*PI4KIII $\beta$  inhibition at 1  $\mu$ M concentration. Chemically, **6**, **8**

and **10** have tertiary amides and lack a H-bond donor at this position. This amide is often a donor in the kinase catalytic site. Further investigations will need to be conducted to establish whether a lack of this donor confers selectivity against *HuPI4KIIIβ*. In the case of **21**, a bulky basic group might clash with Q606 in the ribose pocket of *HuPI4KIIIβ*. A clash with *HuPI4KIIIβ* residue Q606 may serve as a design strategy to achieve the desired selectivity over *HuPI4KIIIβ*.<sup>29</sup>

Toxicity as a result of host kinase off-target inhibition is a risk when designing kinase inhibitors against a pathogen. In the case of *PfPI4K* vs *HuPI4KIIIβ*, there are a few subtle structural differences<sup>29</sup> which may be exploited to achieve effective species selectivity. Therefore, it is likely possible to improve kinase selectivity between species with structure-based modelling against the most relevant host off-targets in parallel with the pathogen on-targets. While *PI4KIIIβ* is likely to be a key off-target for this series, it will also be essential to determine selectivity relative to other human phosphoinositide and protein kinases going forward.

## CONCLUSION

Our study identified new amidated analogues with a combination of good antiparasitoid potency and aqueous solubility. In this regard, analogues **9 – 11**, **19**, **22**, **27** and **29** were found to possess nanomolar antiparasitoid potency ( $IC_{50} = 0.012 - 0.097 \mu M$ ) and high solubility ( $145 - 200 \mu M$ ). Additionally, we have shown that this series potently inhibits *Plasmodium* PI4K, at least as a major target. Interestingly, several compounds also inhibited *Plasmodium* PKG, presenting an opportunity to develop dual PI4K and PKG inhibitors based on the imidazopyridazine scaffold. While multi-kinase inhibitors are often seen in a negative light due to the perception that they are more likely to show activity against human kinase-off-targets, they offer potential advantages including improved efficacy across

the parasite life cycle and reduced propensity for resistance. Our study has also revealed the potential of this series to target multiple stages of parasite development as exemplified by the potent inhibition of early- and late-stage gametocytes by some analogues. To some extent, like multi-kinase inhibition, this property has potential to render this compound class refractory to the development of resistance while ensuring efficacy.

## **METHODS**

### **General Comments on Experimental Data.**

All commercially available chemicals were purchased from either Sigma-Aldrich or Combi-Blocks. All solvents were dried by appropriate techniques. Unless otherwise stated, all solvents used were anhydrous. <sup>1</sup>H-NMR and <sup>13</sup>C-NMR spectra were acquired on either a Bruker AV 400 (<sup>1</sup>H 400.0, <sup>13</sup>C 100.6 MHz), Varian Mercury 300 (<sup>1</sup>H 300.1, <sup>13</sup>C 75.5 MHz) or Bruker Ascend™ 600 (<sup>1</sup>H 600.0, <sup>13</sup>C 151 MHz) spectrometers. An Agilent LC-MS instrument comprising an Agilent 1260® Infinity Binary Pump, Agilent 1260® Infinity Diode Array Detector, Agilent 1290® Infinity Column Compartment, Agilent 1260® Infinity Autosampler, Agilent 6120® Quadrupole MS, and Peak Scientific® Genius 1050 Nitrogen Generator, and fitted with an X-bridge® (C18, 2.5 μm, 3.0 mm (ID) x 50 mm length) column maintained at either 35 or 40 °C was used to monitor the progress of reactions including percent purity determinations. Analytical thin-layer chromatography (TLC) was performed on aluminum-backed silica-gel 60 F<sub>254</sub> (70–230 mesh) plates. Flash column chromatography was performed with Merck silica-gel 60 (70–230 mesh). Chemical shifts (δ) are given in ppm downfield from tetramethylsilane (TMS) as the internal standard. Coupling constants, *J*, are recorded in hertz (Hz). Target compounds were confirmed to have > 95% purity.

**General Procedure for Synthesis of Intermediates 2a and 7a.** The halogenated starting material (**1a** or **6a**) (1.0 equiv), 4-carboxyphenylboronic acid (1.1 equiv) and Pd(PPh<sub>3</sub>)<sub>2</sub>Cl<sub>2</sub> (0.05 equiv) were dissolved in DMF (3 mL/mmol of halogenated starting material). The resulting mixture was flushed with nitrogen for 30 min, after which a 1 M aqueous solution of K<sub>2</sub>CO<sub>3</sub> (1.05 equiv) was added to the reaction mixture. The reaction mixture was heated to 80 °C and stirred for 12 (**2a**) and 15 (**7a**) hours. DMF in the reaction mixture was removed *in vacuo*. The respective intermediate was purified using flash column chromatography using 1% methanol/ethyl acetate acidified with drops of glacial acetic acid as a mobile phase.

*4-(6-Chloroimidazo[1,2-*b*]pyridazin-3-yl)benzoic acid (2a).* Yellow solid (4.42 g, 85%); *R<sub>f</sub>* (CH<sub>3</sub>OH : EtOAc 4 : 96) = 0.38; <sup>1</sup>H-NMR δ<sub>H</sub> (600 MHz, DMSO-*d*<sub>6</sub>) 8.43 (s, 1H), 8.32 (d, *J* = 9.44 Hz, 1H), 8.23 (d, *J* = 8.83 Hz, 2H), 8.08 (d, *J* = 8.83 Hz, 2H), 7.46 (d, *J* = 9.45 Hz, 1H). <sup>13</sup>C-NMR δ<sub>C</sub> (151 MHz, DMSO-*d*<sub>6</sub>) 167.80, 147.02, 139.66, 135.22, 131.94, 131.28, 130.19 (2C), 128.71, 127.44, 126.33 (2C), 119.66; LC-MS, APCI<sup>+</sup>: *m/z* [M + H]<sup>+</sup> = 273.87, calculated exact mass = 273.0305, Purity = 93%, *t<sub>r</sub>* = 2.54 min.

*4-(6-(3-(Methylsulfinyl)phenyl)imidazo[1,2-*b*]pyridazin-3-yl)benzoic acid (3a).* The general procedure for synthesis of intermediates **2a** and **7a** was followed with one modification – the reaction was carried out at 100 °C and left to proceed for 16 hours. Yellow solid (3.56 g, 59%); *R<sub>f</sub>* (CH<sub>3</sub>OH : CH<sub>2</sub>Cl<sub>2</sub> 10 : 90) = 0.36; <sup>1</sup>H-NMR δ<sub>H</sub> (600 MHz, DMSO-*d*<sub>6</sub>) 8.42 (t, *J* = 1.78 Hz, 1H), 8.38 – 8.27 (m, 3H), 8.18 (d, *J* = 8.69 Hz, 2H), 8.05 (d, *J* = 8.55 Hz, 2H), 7.96 (dt, *J* = 8.84, 1.42 Hz, 1H), 7.87 (d, *J* = 9.48 Hz, 1H), 7.81 (t, *J* = 7.68 Hz, 1H), 2.86 (s, 3H); <sup>13</sup>C-NMR δ<sub>C</sub> (151 MHz, DMSO-*d*<sub>6</sub>) 169.65, 150.57, 148.14, 140.66, 139.63, 136.74, 134.20, 130.63, 129.86 (2C), 129.55, 128.79, 128.43, 126.95 (2), 125.60 (2C), 122.52, 116.17, 43.73; LC-MS, APCI<sup>+</sup>: *m/z* [M + H]<sup>+</sup> = 377.8, calculated exact mass = 377.0834, Purity = 95%, *t<sub>r</sub>* = 2.52 min.



6-(3-(Methylsulfonyl)phenyl)imidazo[1,2-*b*]pyridazine (**5a**). A suspension of 6-chloroimidazo[1,2-*b*]pyridazine (**4a**) (3.38 g, 21.9 mmol), 3-methylsulfonylphenylboronic acid (4.84 g, 24.2 mmol), Pd(PPh<sub>3</sub>)<sub>2</sub>Cl<sub>2</sub> (0.772 g, 1.1 mmol) in DMF (61 mL) was purged with nitrogen for 20 min. A 1 M aqueous solution of K<sub>2</sub>CO<sub>3</sub> (3.19 g, 23.1 mmol) was then added. The resulting reaction mixture was left to stir at 100 °C for 19 h. Upon reaction completion, DMF was removed *in vacuo*. The resulting residue was taken up in DCM (300 mL) and washed with saturated NaHCO<sub>3</sub> (aq) (200 mL × 3), H<sub>2</sub>O (200 mL × 3) and saturated NaCl (aq) (200 mL × 3). The organic layer was dried (MgSO<sub>4</sub>) after which the solvent was removed *in vacuo*. The obtained residue was then subjected to column chromatography on silica (0 – 3% CH<sub>3</sub>OH/DCM) to deliver **5a** as a yellow solid (2.62 g, 63%); m.p = 201.9 – 203.9 °C; *R<sub>f</sub>* (CH<sub>3</sub>OH : CH<sub>2</sub>Cl<sub>2</sub> 4 : 96) = 0.54; <sup>1</sup>H-NMR δ<sub>H</sub> (400 MHz, DMSO-*d*<sub>6</sub>) 8.54 (t, *J* = 1.88 Hz, 1H), 8.41 – 8.35 (m, 2H), 8.23 (d, *J* = 9.54 Hz, 1H), 8.07 (dt, *J* = 8.54, 2.69 Hz, 1H), 7.88 (d, *J* = 9.55 Hz, 1H), 7.85 – 7.81 (m, 2H), 3.29 (s, 3H); <sup>13</sup>C-NMR δ<sub>C</sub> (101 MHz, DMSO-*d*<sub>6</sub>) 150.30, 142.14, 138.29, 136.60, 134.87, 132.39, 130.91, 128.73, 126.55, 125.53, 117.86, 116.81, 43.94; LC-MS, APCI<sup>+</sup>: *m/z* [M + H]<sup>+</sup> = 273.9, calculated exact mass = 273.0572, Purity = 98%, *t<sub>r</sub>* = 2.69 min.

3-Iodo-6-(3-(methylsulfonyl)phenyl)imidazo[1,2-*b*]pyridazine (**6a**). 6-(3-(methylsulfonyl)phenyl)imidazo[1,2-*b*]pyridazine (**5a**) (0.670 g, 2.5 mmol) was dissolved in DMF (10 mL), and the mixture was stirred and flushed with nitrogen for 30 min. NIS (0.607 g, 2.7 mmol) was then added in one portion after which the reaction mixture was stirred at 35 °C for 6 days. DMF was then removed *in vacuo*. The obtained residue was taken up in 80 mL DCM and washed with a saturated aqueous solution of sodium metabisulfite (Na<sub>2</sub>S<sub>2</sub>O<sub>5</sub>) (200 mL × 5) and H<sub>2</sub>O (400 mL × 1). The organic layer was dried over MgSO<sub>4</sub> after which DCM was removed *in vacuo* to afford **6a** as a yellow solid (0.855 g, 87%); m.p = 204.3 – 206.3 °C; *R<sub>f</sub>* (CH<sub>3</sub>OH : CH<sub>2</sub>Cl<sub>2</sub> 4 : 96) = 0.68; <sup>1</sup>H-NMR δ<sub>H</sub> (400 MHz, DMSO-*d*<sub>6</sub>) 8.65 (t, *J* = 1.89 Hz,

1H), 8.48 (dt,  $J = 7.86, 1.83$  Hz, 1H), 8.29 (d,  $J = 9.50$  Hz, 1H), 8.13 (dt,  $J = 7.83, 1.85$  Hz, 1H), 8.03 – 7.97 (m, 2H), 7.90 (t,  $J = 7.88$  Hz, 1H), 3.34 (s, 3H);  $^{13}\text{C-NMR}$   $\delta_{\text{C}}$  (101 MHz, DMSO- $d_6$ ) 150.78, 142.41, 141.03 (2C), 136.51, 132.34, 130.89, 128.96, 126.60, 125.75, 117.07, 72.70, 43.97; LC-MS, APCI $^+$ :  $m/z$   $[\text{M} + \text{H}]^+ = 399.6$ , calculated exact mass = 398.9538, Purity = 99.9%,  $t_{\text{r}} = 2.45$  min.

**General Procedure for Synthesis of Amide Target Compounds 5, 6i and 7 – 18.** A mixture of an appropriate carboxylic acid intermediate (1.0 equiv), DIPEA (7.0 equiv) and appropriate amine (3.0 equiv) in either DMF (**5**, **6i**, **7 – 10** and **13 – 18**) or DCM (**11** and **12**) was cooled in ice water while magnetically stirring. A solution of propylphosphonic anhydride solution (50% w/w in ethyl acetate for **13 – 18**; 50% w/w in DMF for **5**, **6i** and **7 – 12**) (4.0 equiv) was added dropwise. The reaction mixture was then left to stir at either room temperature (**11** and **12**) or 50 °C (**5**, **6i**, **7 – 10** and **13 – 18**) for 3 – 6 h. The reaction mixtures for compounds **5**, **6i** and **7 – 12** were then diluted with DCM (25 mL). The resulting mixture was then washed with water (10 mL  $\times$  2) and saturated aqueous solutions of NaHCO $_3$  (10 mL  $\times$  3) and NaCl (10 mL  $\times$  3). The organic layer was dried (Na $_2$ SO $_4$ ) after which it was concentrated *in vacuo*. Following the completion of reaction for compounds **13 – 18**, the solvent was removed *in vacuo*. The crude mixtures for compounds **5** and **7 – 18** were then subjected to further purification by prep-TLC or column chromatography to deliver the title compounds. The *N*-*boc*-protected amide intermediate **6i** was used in the next deprotection step without further purification.

(4-(6-(3-(Methylsulfinyl)phenyl)imidazo[1,2-*b*]pyridazin-3-yl)phenyl)(piperidin-1-yl)methanone (**5**). Purified by prep-TLC (developed in 3% CH $_3$ OH/DCM). Bright yellow solid (0.0468 g, 27.3%);  $R_{\text{f}}$  (CH $_3$ OH : CH $_2$ Cl $_2$  5 : 95) = 0.39;  $^1\text{H-NMR}$   $\delta_{\text{H}}$  (400 MHz, CDCl $_3$ ) 8.40 (s, 1H), 8.32 (s, 1H), 8.22 (m, 2H), 8.17 (d,  $J = 8.11$  Hz, 2H), 7.85 (m, 2H), 7.76 (t,  $J = 7.7$  Hz, 1H), 7.62 (d,  $J = 8.1$  Hz, 2H), 3.77 (s, 2H), 3.50 (m, 2H), 2.84 (s, 3H), 1.81 – 1.58 (m, 6H);

$^{13}\text{C}$ -NMR  $\delta_{\text{C}}$  (151 MHz, Methanol- $d_4$ ) 171.9, 152.3, 147.6, 141.1, 138.2, 136.8, 134.2, 131.5, 131.1, 131.0, 129.4, 128.4 (2C), 127.9 (2C), 127.0, 126.5, 123.4, 117.9, 50.2, 44.4, 43.7, 27.6, 26.8, 25.5; LC-MS, APCI $^+$ :  $m/z$   $[\text{M} + \text{H}]^+ = 445.1$ , calculated exact mass = 444.1620, purity = 99%,  $t_{\text{r}} = 3.48$  min.

*6-Chloro-3-(4-(methylsulfinyl)phenyl)imidazo[1,2-*b*]pyridazine (2b)*. A suspension of 6-chloro-3-iodoimidazo[1,2-*b*]pyridazine (**1a**) (1.0 equiv), 4-methylsulfinylphenylboronic acid (1.1 equiv) and Pd(PPh $_3$ ) $_2$ Cl $_2$  (0.05 equiv) in DMF (3 mL/mmol of **1a**) was purged with nitrogen for 20 minutes. A 1 M aqueous solution of K $_2$ CO $_3$  (1.05 equiv) was then added after which the reaction mixture was heated to 80 °C and left to magnetically stir at that temperature for 14 hours. The reaction mixture was diluted with DCM, washed with deionized water (8  $\times$ ), saturated aqueous solutions of NaHCO $_3$  (3  $\times$ ), NH $_4$ Cl (3  $\times$ ) and NaCl (1  $\times$ ). After drying the organic layer (MgSO $_4$ ), the solvent was removed *in vacuo* and the resulting residue subjected to automated column chromatography on silica (0 – 3% CH $_3$ OH/DCM) to give the chloro-substituted derivative **2b**. Yellow solid (0.587 g, 77%);  $^1\text{H}$ -NMR  $\delta_{\text{H}}$  (300 MHz, CDCl $_3$ ) 8.24 (d,  $J = 8.2$  Hz, 2H), 8.18 (s, 1H), 8.11 (d,  $J = 9.4$  Hz, 1H), 7.82 (d,  $J = 8.0$  Hz, 2H), 7.22 (d,  $J = 8.8$  Hz, 1H), 2.81 (s, 3H); LC-MS, APCI $^+$ :  $m/z$   $[\text{M} + \text{H}]^+ = 292.0$ , calculated exact mass = 291.0233,  $t_{\text{r}} = 3.0$  min.

*3-(3-(4-(Methylsulfinyl)phenyl)imidazo[1,2-*b*]pyridazin-6-yl)benzoic acid (3b)*. Compound **3b** was synthesized according to the procedure described for synthesis of **2a** and **7a** with some minor modifications. The reaction was carried out at 100 °C for 15 h in 1,4-dioxane. Yellow solid (1.263 g, 68%);  $R_{\text{f}}$  (CH $_3$ OH : CH $_2$ Cl $_2$  10 : 90) = 0.15;  $^1\text{H}$ -NMR  $\delta_{\text{H}}$  (600 MHz, DMSO- $d_6$ ) 8.62 (br s, 1H), 8.46 (d,  $J = 8.81$  Hz, 2H), 8.40 (s, 1H), 8.31 (d,  $J = 9.50$  Hz, 1H), 8.25 (dt,  $J = 7.81, 1.8$  Hz, 1H), 8.08 (dt,  $J = 7.69, 1.8$  Hz, 1H), 7.92 (d,  $J = 9.51$  Hz, 1H), 7.83 (d,  $J = 8.81$  Hz, 2H), 7.63 (t,  $J = 7.66$  Hz, 1H), 2.80 (s, 3H);  $^{13}\text{C}$ -NMR  $\delta_{\text{C}}$  (151 MHz, DMSO- $d_6$ ) 168.33, 151.63, 145.78, 140.13, 135.43, 134.91, 131.32, 131.19, 130.22 (3C),

129.52, 128.17 (2C), 127.12 (2C), 127.04, 124.59, 116.96, 43.62; LC-MS, APCI<sup>+</sup>:  $m/z$  [M + H]<sup>+</sup> = 378.0, calculated exact mass = 377.0834, purity = 94%,  $t_r$  = 2.74 min.

**General Procedure for Synthesis of Amide Target Compounds 19, 20, 21i, 22 - 27, 28i, 29 and 30.** A mixture of 3-(3-(4-(methylsulfinyl)phenyl)imidazo[1,2-*b*]pyridazin-6-yl)benzoic acid (**3b**) (1.0 equiv), DIPEA (7.0 equiv) and appropriate amine (3.0 equiv) in either DMF (**19, 20, 21i, 26 - 27** and **28i**) or 1,4-dioxane (**22 - 25, 29** and **30**) was cooled in ice water while magnetically stirring. A solution of propylphosphonic anhydride solution (50% w/w in ethyl acetate) (4.0 equiv) was added dropwise. The reaction mixture was then left to stir at either 30 °C (**22 - 25, 29** and **30**) or 50 °C (**19, 20, 21i, 26 - 27** and **28i**) for 1 - 21 h. Following the completion of reaction, the solvent was removed *in vacuo*. The crude mixtures were then subjected to further purification by prep-TLC or column chromatography to deliver the title compounds. The *N*-*boc*-protected amide intermediates **21i** and **28i** were used in the next deprotection step without further purification.

*N*-(2-Hydroxyethyl)-3-(3-(4-(methylsulfinyl)phenyl)imidazo[1,2-*b*]pyridazin-6-yl)benzamide (**19**). Purified by prep-TLC (developed in 0-10% CH<sub>3</sub>OH/DCM with a few drops of 7 M aqueous ammonia). Yellow solid (0.0034 g, 4%);  $R_f$  (CH<sub>3</sub>OH : CH<sub>2</sub>Cl<sub>2</sub> 10 : 90) = 0.34; <sup>1</sup>H-NMR  $\delta_H$  (300 MHz, DMSO-*d*<sub>6</sub>) 8.67 (t,  $J$  = 5.53 Hz, 1H), 8.59 (t,  $J$  = 1.84 Hz, 1H), 8.50 (d,  $J$  = 8.41 Hz, 2H), 8.44 (s, 1H), 8.40 (d,  $J$  = 9.54 Hz, 1H), 8.32 (dt,  $J$  = 7.80, 1.8 Hz, 1H), 8.07 - 7.97 (m, 2H), 7.88 (d,  $J$  = 8.40 Hz, 2H), 7.71 (t,  $J$  = 7.76 Hz, 1H), 4.76 (t,  $J$  = 5.55 Hz, 1H), 3.58 (q,  $J$  = 5.95 Hz, 2H), 3.41 (q,  $J$  = 5.81 Hz, 2H), 2.83 (s, 3H); <sup>13</sup>C-NMR  $\delta_C$  (151 MHz, DMSO-*d*<sub>6</sub>) 166.29, 151.39, 145.83, 140.14, 135.92, 135.59, 134.98, 131.13, 129.96, 129.77, 129.52 (2C), 127.19 (2C), 127.16, 127.08, 126.37, 124.64, 116.92, 60.24, 43.64, 42.78; LC-MS, APCI<sup>+</sup>:  $m/z$  [M + H]<sup>+</sup> = 421.1, calculated exact mass = 420.1256, purity = 96%,  $t_r$  = 3.36 min.

**General Procedure for Synthesis of Compounds 21 and 28.** Compounds **21** and **28** were synthesized following the procedure already described for the synthesis of compound **6** with a minor modification – these deprotection steps were carried out in the presence of 4 M HCl in 1,4-dioxane, with DCM as the solvent.

(3-(3-(4-(Methylsulfinyl)phenyl)imidazo[1,2-*b*]pyridazin-6-yl)phenyl)(piperazin-1-yl)methanone (**28**). Purified by prep-TLC (developed in 0-10% CH<sub>3</sub>OH/DCM with a few drops of 7 M aqueous ammonia). Pale yellow solid (0.010 g, 20%); *R<sub>f</sub>* (CH<sub>3</sub>OH : CH<sub>2</sub>Cl<sub>2</sub> 3 : 97) = 0.12; <sup>1</sup>H-NMR δ<sub>H</sub> (300 MHz, Methanol-*d*<sub>4</sub>) 8.21 (dt, *J* = 7.8, 1.6 Hz, 1H), 8.16 - 8.08 (m, 5H), 7.84 (d, *J* = 9.5 Hz, 1H), 7.69 (t, *J* = 7.7 Hz, 1H), 7.61 (dt, *J* = 7.7, 1.5 Hz, 1H), 7.41 (d, *J* = 8.5 Hz, 2H), 3.98 - 3.46 (m, 4H), 3.12 - 2.76 (m, 4H), 2.56 (s, 3H); <sup>13</sup>C-NMR δ<sub>C</sub> (101 MHz, Methanol-*d*<sub>4</sub>) 168.88, 161.22, 142.37, 139.58, 135.46, 135.26, 132.90, 128.48 (2C), 128.22 (2C), 127.68, 127.38, 127.12, 126.21, 125.73 (2C), 125.69, 124.52, 116.90, 54.63 (2C), 48.21 (2C); LC-MS, APCI<sup>+</sup>: *m/z* [M + H]<sup>+</sup> = 446.1, calculated exact mass = 445.1572, purity = 99.9%, *t<sub>r</sub>* = 2.12 min.

## ASSOCIATED CONTENT

### Supporting Information

The Supporting Information is available free of charge on the ACS Publications website at DOI:

- Synthetic methods and characterization data for some compounds (**6**, **7a**, **7 – 18**, **20 – 27**, **29** and **30**); <sup>1</sup>H-NMR spectra for selected compounds; methods for *in vitro* asexual blood stage antiplasmodium evaluation, solubility determination, *in vitro* PvPI4K, PfpKG and HuPI4KIIIβ inhibition assays and *in silico* docking, hERG inhibition and cytotoxicity assays, *in vitro* activities against early- and late-

stage gametocytes; % gametocyte inhibition data; K1 IC<sub>50</sub> values for compounds 5 – 12 and 14 – 18; hERG and cytotoxicity data for selected compounds (PDF).

- Molecular formula strings (CSV).

## **AUTHOR INFORMATION**

### **Corresponding author**

\*(K.C.) E-mail: kelly.chibale@uct.ac.za. Phone: +27-21-6502553. Fax: +27-21-6505195.

### **Author Contributions**

The first authorship is equally shared between P.M.C. and L.C. All other authors contributed to the design of experiments, preparation and proof-reading of the manuscript. All authors read and approved the manuscript for publication.

### **Notes**

The authors declare no competing interest.

## **ACKNOWLEDGMENTS**

We gratefully acknowledge the support of the University of Cape Town, South African Medical Research Council and the South African Research Chairs Initiative of the Department of Science and Innovation administered through the South African National Research Foundation (K.C. and L.B., UID84627). We acknowledge the South African National Research Foundation for the Community of Practice grant (UID 110666). At Swiss TPH, we thank Christoph Fischli, Christin Gump, Sibylle Sax and Christian Scheurer for assistance in performing the antimalarial assays. The FLAIR Fellowship Programme, a partnership between the African Academy of Sciences and the Royal Society funded by the UK Government's Global Challenges Research Fund (GCRF) and the GCRF Synchrotron Techniques for African Research and Technology (START) program is also gratefully acknowledged (L.B.A).

## ABBREVIATIONS USED

cGMP, cyclic guanine monophosphate; PKG, cyclic guanine monophosphate (cGMP)-dependent protein kinase; PI4K, phosphatidylinositol-4-kinase; ATP, adenosine triphosphate; hERG, human *ether-a-go-go*-related gene; IC<sub>50</sub>, concentration of a drug that is required for 50% inhibition *in vitro*; *P. falciparum*, *Plasmodium falciparum*; *P. f.*, *Plasmodium falciparum*; Inh, inhibition; SI, selectivity index; CHO, Chinese hamster ovarian; WHO, World Health Organization; ACT, artemisinin combination therapy; PDB, protein data base; Val, valine; Lys, lysine; Asp, aspartic acid; Ser, serine; Phe, phenylalanine; Thr, threonine; Glu, glutamic acid; Arg, arginine; *P. berghei*, *Plasmodium berghei*; MSD, mean survival days; DIPEA, diisopropylethylamine; T3P, n-propylphosphonic anhydride; SAR, structure-activity relationship; NIS, *N*-iodosuccinimide; DMF, *N,N*-dimethylformamide; rt, room temperature; SD, standard deviation; ND, not determined; TLC, thin layer chromatography; HPLC, high pressure liquid chromatography; LC-MS, liquid chromatography mass spectrometry; UV, ultraviolet; ESI, electrospray ionisation; APCI, atmospheric pressure chemical ionization; <sup>1</sup>H-NMR, proton nuclear magnetic resonance; <sup>13</sup>C-NMR, carbon-13 nuclear magnetic resonance; TMS, tetramethylsilane; DCM, dichloromethane; DMSO, dimethyl sulfoxide; DMSO-d<sub>6</sub>, deuterated dimethyl sulfoxide; t<sub>r</sub>, retention time; R<sub>f</sub>, retardation factor; m.p., melting point; δ<sub>H</sub>, chemical shift in <sup>1</sup>H-NMR spectrum; δ<sub>C</sub>, chemical shift in <sup>13</sup>C-NMR spectrum; *m/z*, mass to charge ratio; EG, early-stage gametocytes; LG, late-stage gametocytes.

## REFERENCES

- (1) World Health Organization. *World Malaria Report*; 2019. <https://www.who.int/publications/i/item/9789241565721>.
- (2) White, N. J. Antimalarial Drug Resistance. *J. Clin. Invest.* **2004**, *113*, 1084–1092.
- (3) Sibley, C. H.; Hyde, J. E.; Sims, P. F.; Plowe, C. V.; Kublin, J. G.; Mberu, E. K.;

- Cowman, A. F.; Winstanley, P. A.; Watkins, W. M.; Nzila, A. M. Pyrimethamine–Sulfadoxine Resistance in Plasmodium Falciparum: What Next? *Trends Parasitol.* **2001**, *17*, 570–571.
- (4) Terlouw, D. J.; Nahlen, B. L.; Courval, J. M.; Kariuki, S. K.; Rosenberg, O. S.; Oloo, A. J.; Kolczak, M. S.; Hawley, W. A.; Lal, A. A.; Kuile, F. O. T. Sulfadoxine-Pyrimethamine in Treatment of Malaria in Western Kenya: Increasing Resistance and Underdosing. *Antimicrob. Agents Chemother.* **2003**, *47*, 2929–2932.
- (5) Warhurst, D. C. Resistance to Antifolates in Plasmodium Falciparum, the Causative Agent of Tropical Malaria. *Sci. Prog.* **2002**, *85*, 89–111.
- (6) Uwimana, A.; Legrand, E.; Stokes, B. H.; Ndikumana, J.-L. M.; Warsame, M.; Umulisa, N.; Ngamije, D.; Munyaneza, T.; Mazarati, J.-B.; Munguti, K.; Campagne, P.; Criscuolo, A.; Ariey, F.; Murindahabi, M.; Ringwald, P.; Fidock, D. A.; Mbituyumuremyi, A.; Menard, D. Emergence and Clonal Expansion of in Vitro Artemisinin-Resistant Plasmodium Falciparum Kelch13 R561H Mutant Parasites in Rwanda. *Nat. Med.* **2020**. <https://doi.org/10.1038/s41591-020-1005-2>.
- (7) Kusakabe, K.-I.; Yoshida, H.; Nozu, K.; Hashizume, H.; Tadano, G.; Sato, J.; Tamura, Y.; Mitsuoka, Y. Imidazo[1,2- b]Pyridazine and Pyrazolo[1,5-a]Pyrimidine Derivatives and Their Use as Protein Kinase Inhibitors. WO2011/013729A1, 2011.
- (8) Xu, Y.; Brenning, B. G.; Kultgen, S. G.; Liu, X.; Saunders, M.; Ho, K.-K. Preparation of Imidazo[1,2-b]Pyridazine and Pyrazolo[1,5- a]Pyrimidine Derivatives as Protein Kinase Inhibitors. US20120058997, 2012.
- (9) Moran, D. B.; Powell, D. W.; Albright, J. D. Imidazo[1,2-b]Pyridazines. US4569934A, 1986.
- (10) Matsumoto, S.; Miyamoto, N.; Hirayama, T.; Oki, H.; Okada, K.; Tawada, M.; Iwata, H.; Nakamura, K.; Yamasaki, S.; Miki, H.; Hori, A.; Imamura, S. Structure-Based



Design, Synthesis, and Evaluation of Imidazo[1,2-b]Pyridazine and Imidazo[1,2-a]Pyridine Derivatives as Novel Dual c-Met and VEGFR2 Kinase Inhibitors. *Bioorg. Med. Chem.* **2013**, *21*, 7686–7698.

- (11) Osborne, S.; Chapman, T.; Large, J.; Bouloc, N.; Wallace, C. Fused Heterocyclic Compounds for Use in the Treatment of Malaria. WO 2011101640, 2011.
- (12) Lemercier, G.; Fernandez-Montalvan, A.; Shaw, J. P.; Kugelstadt, D.; Bomke, J.; Domostoj, M.; Schwarz, M. K.; Scheer, A.; Kappes, B.; Leroy, D. Identification and Characterization of Novel Small Molecules as Potent Inhibitors of the Plasmodial Calcium-Dependent Protein Kinase 1. *Biochemistry* **2009**, *48*, 6379–6389.
- (13) Sahu, N. K.; Kohli, D. V. Structural Insight for Imidazopyridazines as Malarial Kinase PfPK7 Inhibitors Using QSAR Techniques. *Med. Chem. (Los. Angeles)*. **2012**, *8*, 636–648.
- (14) McNamara, C. W.; Lee, M. C. S.; Lim, C. S.; Lim, S. H.; Roland, J.; Nagle, A.; Simon, O.; Yeung, B. K. S.; Chatterjee, A. K.; McCormack, S. L.; Manary, M. J.; Zeeman, A.-M.; Dechering, K. J.; Kumar, T. R. S.; Henrich, P. P.; Gagaring, K.; Ibanez, M.; Kato, N.; Kuhen, K. L.; Fischli, C.; Rottmann, M.; Plouffe, D. M.; Bursulaya, B.; Meister, S.; Rameh, L.; Trappe, J.; Haasen, D.; Timmerman, M.; Sauerwein, R. W.; Suwanarusk, R.; Russell, B.; Renia, L.; Nosten, F.; Tully, D. C.; Kocken, C. H. M.; Glynn, R. J.; Bodenreider, C.; Fidock, D. A.; Diagana, T. T.; Winzeler, E. A. Targeting Plasmodium PI(4)K to Eliminate Malaria. *Nature* **2013**, *504*, 248–253.
- (15) Green, J. L.; Moon, R. W.; Whalley, D.; Bowyer, P. W.; Wallace, C.; Rochani, A.; Nageshan, R. K.; Howell, S. A.; Grainger, M.; Jones, H. M.; Ansell, K. H.; Chapman, T. M.; Taylor, D. L.; Osborne, S. A.; Baker, D. A.; Tatu, U.; Holder, A. A. Imidazopyridazine Inhibitors of Plasmodium Falciparum Calcium-Dependent Protein Kinase 1 Also Target Cyclic GMP-Dependent Protein Kinase and Heat Shock Protein

- 90 To Kill the Parasite at Different Stages of Intracellular Development. *Antimicrob. Agents Chemother.* **2016**, *60*, 1464–1475.
- (16) Paquet, T.; Le Manach, C.; Cabrera, D. G.; Younis, Y.; Henrich, P. P.; Abraham, T. S.; Lee, M. C. S.; Basak, R.; Ghidelli-Disse, S.; Lafuente-Monasterio, M. J.; Bantscheff, M.; Ruecker, A.; Blagborough, A. M.; Zakutansky, S. E.; Zeeman, A.-M.; White, K. L.; Shackelford, D. M.; Mannila, J.; Morizzi, J.; Scheurer, C.; Angulo-Barturen, I.; Martínez, M. S.; Ferrer, S.; Sanz, L. M.; Gamo, F. J.; Reader, J.; Botha, M.; Dechering, K. J.; Sauerwein, R. W.; Tungtaeng, A.; Vanachayangkul, P.; Lim, C. S.; Burrows, J.; Witty, M. J.; Marsh, K. C.; Bodenreider, C.; Rochford, R.; Solapure, S. M.; Jiménez-Díaz, M. B.; Wittlin, S.; Charman, S. A.; Donini, C.; Campo, B.; Birkholtz, L.-M.; Hanson, K. K.; Drewes, G.; Kocken, C. H. M.; Delves, M. J.; Leroy, D.; Fidock, D. A.; Waterson, D.; Street, L. J.; Chibale, K. Antimalarial Efficacy of MMV390048, an Inhibitor of Plasmodium Phosphatidylinositol 4-Kinase. *Sci. Transl. Med.* **2017**, *9*, eaad9735.
- (17) Baker, D. A.; Stewart, L. B.; Large, J. M.; Bowyer, P. W.; Ansell, K. H.; Jiménez-Díaz, M. B.; El Bakkouri, M.; Birchall, K.; Dechering, K. J.; Bouloc, N. S.; Coombs, P. J.; Whalley, D.; Harding, D. J.; Smiljanic-Hurley, E.; Wheldon, M. C.; Walker, E. M.; Dessens, J. T.; Lafuente, M. J.; Sanz, L. M.; Gamo, F.-J.; Ferrer, S. B.; Hui, R.; Bousema, T.; Angulo-Barturén, I.; Merritt, A. T.; Croft, S. L.; Gutteridge, W. E.; Kettleborough, C. A.; Osborne, S. A. A Potent Series Targeting the Malarial CGMP-Dependent Protein Kinase Clears Infection and Blocks Transmission. *Nat. Commun.* **2017**, *8*, 430.
- (18) Vanaerschot, M.; Murithi, J. M.; Pasaje, C. F. A.; Ghidelli-Disse, S.; Dwomoh, L.; Bird, M.; Spottiswoode, N.; Mittal, N.; Arendse, L. B.; Owen, E. S.; Wicht, K. J.; Siciliano, G.; Bösche, M.; Yeo, T.; Kumar, T. R. S.; Mok, S.; Carpenter, E. F.; Giddins, M. J.;

- Sanz, O.; Otilie, S.; Alano, P.; Chibale, K.; Llinás, M.; Uhlemann, A.-C.; Delves, M.; Tobin, A. B.; Doerig, C.; Winzeler, E. A.; Lee, M. C. S.; Niles, J. C.; Fidock, D. A. Inhibition of Resistance-Refractory *P. Falciparum* Kinase PKG Delivers Prophylactic, Blood Stage, and Transmission-Blocking Antiplasmodial Activity. *Cell Chem. Biol.* **2020**, *27*, 806-816.e8.
- (19) Sinxadi, P.; Donini, C.; Johnstone, H.; Langdon, G.; Wiesner, L.; Allen, E.; Duparc, S.; Chalon, S.; McCarthy, J. S.; Lorch, U.; Chibale, K.; Möhrle, J.; Barnes, K. I. Safety, Tolerability, Pharmacokinetics, and Antimalarial Activity of the Novel Plasmodium Phosphatidylinositol 4-Kinase Inhibitor MMV390048 in Healthy Volunteers. *Antimicrob. Agents Chemother.* **2020**, *64*, e01896-19.
- (20) Le Manach, C.; González Cabrera, D.; Douelle, F.; Nchinda, A. T.; Younis, Y.; Taylor, D.; Wiesner, L.; White, K. L.; Ryan, E.; March, C.; Duffy, S.; Avery, V. M.; Waterson, D.; Witty, M. J.; Wittlin, S.; Charman, S. A.; Street, L. J.; Chibale, K. Medicinal Chemistry Optimization of Antiplasmodial Imidazopyridazine Hits from High Throughput Screening of a SoftFocus Kinase Library: Part 1. *J. Med. Chem.* **2014**, *57*, 2789–2798.
- (21) Cheuka, P. M.; Lawrence, N.; Taylor, D.; Wittlin, S.; Chibale, K. Antiplasmodial Imidazopyridazines: Structure–Activity Relationship Studies Lead to the Identification of Analogues with Improved Solubility and HERG Profiles. *Medchemcomm* **2018**, *9*, 1733–1745.
- (22) Le Manach, C.; Paquet, T.; González Cabrera, D.; Younis, Y.; Taylor, D.; Wiesner, L.; Lawrence, N.; Schwager, S.; Waterson, D.; Witty, M. J.; Wittlin, S.; Street, L. J.; Chibale, K. Medicinal Chemistry Optimization of Antiplasmodial Imidazopyridazine Hits from High Throughput Screening of a SoftFocus Kinase Library: Part 2. *J. Med. Chem.* **2014**, *57*, 8839–8848.

- (23) Kingsbury, C. A. Why are the Nitro and Sulfone Groups Poor Hydrogen Bonders? <https://digitalcommons.unl.edu/cgi/viewcontent.cgi?referer=https://www.google.co.za/&httpsredir=1&article=1080&context=chemfacpub>. Accessed: 2018-07-18. (Archived by WebCite® at <http://www.webcitation.org/7107YWmgd>).
- (24) Wissmann, H.; Kleiner, H.-J. New Peptide Synthesis. *Angew. Chemie Int. Ed. English* **1980**, *19*, 133–134.
- (25) Srinivasan, N.; Yurek-George, A.; Ganesan, A. Rapid Deprotection of N-Boc Amines by TFA Combined with Freebase Generation Using Basic Ion-Exchange Resins. *Mol. Divers.* **2005**, *9*, 291–293.
- (26) Wilbek, T. S.; Skovgaard, T.; Sorrell, F. J.; Knapp, S.; Berthelsen, J.; Strømgaard, K. Identification and Characterization of a Small-Molecule Inhibitor of Death-Associated Protein Kinase 1. *ChemBioChem* **2015**, *16*, 59–63.
- (27) Choi, H.-S.; Rucker, P. V.; Wang, Z.; Fan, Y.; Albaugh, P.; Chopiuk, G.; Gessier, F.; Sun, F.; Adrian, F.; Liu, G.; Hood, T.; Li, N.; Jia, Y.; Che, J.; McCormack, S.; Li, A.; Li, J.; Steffy, A.; Culazzo, A.; Tompkins, C.; Phung, V.; Kreusch, A.; Lu, M.; Hu, B.; Chaudhary, A.; Prashad, M.; Tuntland, T.; Liu, B.; Harris, J.; Seidel, H. M.; Loren, J.; Molteni, V. (R)-2-Phenylpyrrolidine Substituted Imidazopyridazines: A New Class of Potent and Selective Pan-TRK Inhibitors. *ACS Med. Chem. Lett.* **2015**, *6*, 562–567.
- (28) Merckx, A.; Echalié, A.; Langford, K.; Sicard, A.; Langsley, G.; Joore, J.; Doerig, C.; Noble, M.; Endicott, J. Structures of P. Falciparum Protein Kinase 7 Identify an Activation Motif and Leads for Inhibitor Design. *Structure* **2008**, *16*, 228–238.
- (29) Fienberg, S.; Eyermann, C. J.; Arendse, L.; Basarab, G. S.; McPhail, J.; Burke, J. E.; Chibale, K. Structural Basis for Inhibitor Potency and Selectivity of Plasmodium Falciparum Phosphatidylinositol 4-Kinase Inhibitors. *ACS Infect. Dis.* **2020**, [acsinfecdis.0c00566](https://doi.org/10.1021/acsinfecdis.0c00566). <https://doi.org/10.1021/acsinfecdis.0c00566>.

- (30) Cabrera, D. G.; Horatscheck, A.; Wilson, C. R.; Basarab, G.; Eyermann, C. J.; Chibale, K. Plasmodial Kinase Inhibitors: License to Cure? *J. Med. Chem.* **2018**, *61*, 8061–8077.
- (31) El Bakkouri, M.; Kouidmi, I.; Wernimont, A. K.; Amani, M.; Hutchinson, A.; Loppnau, P.; Kim, J. J.; Flueck, C.; Walker, J. R.; Seitova, A.; Senisterra, G.; Kakihara, Y.; Kim, C.; Blackman, M. J.; Calmettes, C.; Baker, D. A.; Hui, R. Structures of the CGMP-Dependent Protein Kinase in Malaria Parasites Reveal a Unique Structural Relay Mechanism for Activation. *Proc. Natl. Acad. Sci.* **2019**, *116*, 14164–14173.
- (32) Burke, J. E. Structural Basis for Regulation of Phosphoinositide Kinases and Their Involvement in Human Disease. *Mol. Cell* **2018**, *71*, 653–673.
- (33) Miller, M.; Thompson, P.; Gabelli, S. Structural Determinants of Isoform Selectivity in PI3K Inhibitors. *Biomolecules* **2019**, *9*, 82.